Supporting Information

Xie et al. 10.1073/pnas.0910055107

SI Materials and Methods

Media, Bacterial Strains, and Growth Conditions. The *A. brasilense* cells were grown at 28 °C in a minimal medium (MMAB) (1) supplemented with the carbon source of choice at a final concentration of 10 mM. Strains are listed in Table S2. Cells were grown in MMAB with ammonium as the combined nitrogen source under aerobic conditions (200 rpm on a rotary shaker) or under microaerophilic conditions (static cultures) without combined nitrogen source (nitrogen fixation conditions). For anaerobic growth, cells were incubated in a GasPak anaerobic system (Becton Dickinson) with 10 mM sodium nitrate as a terminal electron acceptor. The growth medium was supplemented with the antibiotics kanamycin (30 μg/mL), tetracycline (10 μg/mL), and spectinomycin (60 μg/mL) when required for plasmid maintenance.

Mutant Constructions and Complementation. All strains and plasmids used are listed in Table S2. Preparation of plasmid and genomic DNA, transformations, restriction endonuclease digestions, DNA extraction from agarose gels, ligation reactions, PCR and Southern hybridization, and DNA transformation into *E. coli* were carried out by standard protocols and the manufacturers' instructions. The enzymes for DNA manipulation and PCR amplification were purchased from New England Biolabs and Epicentre. Construction of the *ΔaerC* mutant strain was as follows: A 713-bp fragment directly upstream of *aerC* and containing the start codon was amplified from the genomic DNA of *A. brasilense* Sp7 using the primer pair tlp3UF and tlp3UR (Table S3). A 699-bp fragment directly downstream of *aerC* and encompassing the stop codon and 491 bp at the 3′ end of the gene was amplified from the genomic DNA of the wild-type strain using the primer pair tlp3DF and tlp3DR (Table S3). Individual fragments were cloned into the pCR2.1 TOPO vector (Invitrogen), yielding pCR*aerC*U and pCR*aerC*D, respectively, and sequenced. The upstream and downstream fragments were subsequently isolated from these vectors by digestion with NcoI and NotI (upstream fragment) and ApaI and SacI (downstream fragment) before being cloned into corresponding restriction sites in the pCM184 vector. In the resulting construct (pCM*aerCUD*::Kan), the kanamycin cassette from pCM184 is inserted in-frame between the two cloned fragments, yielding a Δ*aerC::kan* construct. The entire Δ*aerC::kan* construct was amplified using the primers tlp3UF and tlp3DR and blunt cloned into the pKNOCKTc suicide vector (digested with SmaI and dephosphorylated with calf intestinal phosphatase, NEBiolabs), yielding pKN*aerC*UD::Kan (Table S2). The construct was verified by restriction digestion and sequencing and transformed into competent *E. coli* EC100*pyr* cells (Epicentre). The *E. coli* EC100*pyr* cells carrying the suicide vector were used for allelic exchange in triparental matings with *A. brasilense* Sp7 as the recipient strain and *E. coli* HB101 (pRK2013) as the helper strain (2). For complementation, the *aerC* ORF and 534 bp of upstream noncoding sequence were amplified by PCR using primers tlp3comF and tlp3comR (Table S3). This 2022-bp *aerC* region was cloned as an ApaI–SpeI fragment into the broad-host-range vector pRK415, yielding pRKAerC. *E. coli* S17-1 competent cells were transformed with pRKAerC and an empty pRK415 vector as negative control which were then used as donors in biparental matings with wild-type *A. brasilense* strain Sp7 and strain AB301, as described previously (3). Site-directed mutagenesis of conserved tryptophan residues in the PAS1 and PAS2 domains of AerC (W77 and W199) was performed using the Quickchange site-directed mutagenesis kit (Stratagene). Mutagenic primers were designed per the manufacturer's instructions (Table S3) using *aerC* cloned in a pUC18 vector as a template (Table S2). The resulting plasmids expressing the full-length and mutagenized *aerC* alleles were digested by the restriction enzymes HindIII and XbaI. These fragments were then individually cloned into broad-host-range vector pRK415 at the appropriate restriction sites, yielding pRKAerC^{W77F}, pRKAerC^{W199F}, and pRKAerC^{W77FW199F} (Table S2).

Generation of AerC–*yfp* Fusions and Fluorescence Microscopy. Plasmids allowing expression of translational fusions of AerC with a C-terminal fusion to Yfp were constructed using Gateway vectors described by Hallez et al. (4). The entry clones were obtained via BP reaction in pDONR221 according to manufacturer's instructions (Invitrogen). A 2,062-bp DNA fragment including the ORF for AerC lacking the stop codon and including 534 bp of the 5′ sequence upstream of the AerC translational start was amplified by PCR and cloned into pDONR221 using the primers GWTlp3F and GWTlp3R (Table S3). Similar constructs were obtained using aerC^{W77F}, aerC^{W199F}, and aerC^{W77FW199F} as templates to generate pDONR*aerC*, pDONR*aerC*^{W77F}, pDONR*aerC*^{W199F}, and pDONR*aerC*^{W77FW199F} entry clones (Table S2). The entry clones were recombined in vitro into the destination vector pRH005 (5) in an LR reaction performed per the manufacturer's instructions (Invitrogen), yielding pRHAerC, pRHAerC^{W77F}, pRHAerC^{W199F}, pRHAerC^{W77FW199F} destination vectors (Table S2). All clones were verified via restriction analysis and sequencing before the LR reaction. The destination vectors were electroporated into *E. coli* OmniMAX2-T1^{R} and selected on Luria-Bertani plates supplemented with kanamycin and chloramphenicol. Recombinant plasmids pRHAerC, pRHAerC^{W77F}, pRHAerC^{W199F}, pRHAerC^{W77FW199F} were transferred by conjugation into *A. brasilense* strains (5).

Total Cellular FAD Content. Total cellular FAD was extracted either from cells grown in MMAB with ammonium or under nitrogen fixation conditions as well as from *A. brasilense* cells overexpressing AerC–Yfp from a medium copy plasmid (pRH005, pRHAerC, pRHAerC^{W77F}, pRHAerC^{W199F}, pRHAerC^{W77FW199F}) essentially as described previously (6). Overexpression from this vector was chosen to facilitate detection of overexpression (by fluorescence) and to ensure proper recombinant protein folding. For determining total cellular FAD content upon overexpression of wild-type and mutant versions of AerC, cultures grown in MMAB under conditions of nitrogen fixation were used. Total FAD was extracted from cell pellets in perchloric acid, and the amount of FAD in cell extracts was determined by detecting photon emission by apo-d-amino acid oxidase in the prereaction buffer (23 mM D-alanine, 7.5 μg horseradish peroxidase, and 25 μM luminal) at 37 °C. Luminescence was counted for 0.1 s every 60 s for 60 min in a POLARstar OPTIMA luminometer (BMG LRBTECH). Peak luminometric readings (≈16 min) were plotted on a standard curve of FAD ranging from 10 fmol to 100 fmol.

β-Glucuronidase Assay for Promoter Activity. A 651-bp fragment at the 5′ region of *aerC* and containing the putative promoter region and the start codon was amplified from the pCR*aerC*UD vector using the primers Tlp3UFNcoI and Tlp3REcoRI (Table S3). The *aerC* DNA region was excised after digestion with HindIII and XhoI and inserted into the pFUS1 promoter probe vector at the appropriate restriction sites (7) to generate translational fusion with the promoterless *gusA* gene present on the

vector (P*aerC-gusA*) and yielding pFUSP*aerC* (Table S2). The proper orientation of the insert relative to the promoterless *gusA* gene was verified by restriction analysis and sequencing. Next, the recombinant vectors pFUSP*aerC* and pFUS1 (negative control) were transformed into competent *E. coli* S17-1 cells and transferred conjugally to *A. brasilense* strain Sp7 as described previously. The *nifH* promoter activity was measured from a P*nifH–gusA* transcriptional fusion carried on a low-copy vector (Table S2), pFAJ318 (8). The plasmid pFAJ318 was transferred by conjugation into *A. brasilense* strains wild type and AB301.

The β-glucuronidase activity was measured from cultures grown at 28 °C either aerobically with shaking in MMAB (with malate 10mM and NH4Cl, 35mM) or in nitrogen-free MMAB under static conditions (nitrogen-fixation conditions) and containing tetracycline for plasmid maintenance. Cultures were grown to mid-to-late exponential phase and harvested by centrifugation (3,500 rpm, 3 min; Eppendorf centrifuge 5417R). The supernatant was removed and cell pellets were stored at −80 °C until β-glucuronidase activity was measured using the method described by Reeve et al. (7). Briefly, the β-glucuronidase activity was measured fluorometrically by monitoring the cleavage of 4-methyl-umbelliferyl β-D-glucuronide (Sigma-Aldrich) to 4-methyl-umbelliferone and glucuronic acid with a Turner 450 Fluorometer. Protein concentration was determined by the Bradford assay (Bio-Rad).

Behavioral Assays. Semisoft plates containing MMAB minimal medium with different carbon source and appropriate antibiotics were inoculated with 5-μL droplets of the test culture adjusted to the same cell density (estimated by OD_{600} nm measurements) and incubated at 28 °C for 3 days. Taxis on swarm plates under anaerobic conditions was assessed with 5 mM nitrate as a terminal electron acceptor using in a GasPak anaerobic system (Becton Dickinson Microbiology Systems and using cells previously grown anaerobically with nitrate as a terminal electron acceptor and adjusted to the same density as evaluated by OD_{600} measurements. There was no detectable difference in the doubling times of the strains under the growth conditions tested (120 min in the presence of ammonium and 170 min under conditions of nitrogen fixation); the rate of expansion of the chemotactic rings can thus be attributed to differences in the ability to navigate the gradients by chemo- or aerotaxis. The capillary assays were performed essentially as previously described (1). Cells were grown in nitrogen-free MMAB to exponential phase and washed three times with chemotaxis buffer [10 mM phosphate buffer (pH 7.0), 1 mM EDTA]. Cells were resuspended in chemotaxis buffer with 10 mM malate as carbon source and introduced into an optically flat capillary tube (inner dimensions, 0.1 by 2 by 50 mm; Vitro Dynamics). The position of the aerotactic band formed within 5 min in the capillary tube was compared by measuring the relative distance of the aerotactic band from the meniscus. At least three independent experiments were performed. The temporal gradient assay for aerotaxis was used to measure the response time to adaptation to oxygen removal and was performed as described by Alexandre et al. (1). The miniplug assay for redoxtaxis were performed essentially as previously described with minor modifications (1). A small 1.5% agarose plug in chemotaxis buffer containing the chemical to be tested as a chemoeffector was placed in a microchamber; 200 μL of cell suspension of *A. brasilense* in chemotaxis buffer was introduced in the microchamber and covered with a coverslip. The formation of a band of motile cells away from (repellent effect) the plug was observed and videorecorded using a dark-field video microscope. Different concentrations of a fresh stock solution of 1,4-benzoquinone in DMSO were introduced into the plug to determine the threshold for repellent response. Plugs containing the substituted quinone were supplemented with 2 mM ferricyanide to maintain the quinones in an oxidized state and control plugs containing DMSO or ferricyanide were also introduced in the same microchamber. Ferricyanide alone or DMSO alone did not affect bacterial behavior.

Western Blots. Bacterial cells grown in MMAB minimal medium with 10 mM malate as carbon source were harvested and washed once with PBS and resuspended in 0.4 mL of PBS. Or cells were induced overnight above minimal medium without nitrogen source. The cells were disrupted by sonication. Cell debris was removed by centrifugation at 20,800 × *g* for 10 min at 4 °C. Protein concentrations were determined by the BCA method (Pierce) according to manufacturer's instructions. A cell lysate (10 μg of protein) was run in an SDS-15% polyacrylamide gel, and transferred onto a nitrocellulose membrane. Immunoblots were carried out with the purified primary $Aer_{2–166}$ antibody at a 1:100 dilution (Crude $Aer_{2–166}$ antibody, kindly supplied by K. Watts and B. L. Taylor) or an anti-GFP antibody (which crossreacts with Yfp, a gift from R. Goodchild) at a 1:1,000 dilution in TBS-T with 1.0% nonfat dry milk. The $Aer_{2–166}$ antibody was purified using nickel NTA affinity chromatography (Qiagen) according to the manufacturer's protocol. The membrane was incubated overnight at room temperature, washed three times with PBS-T, and incubated with the HRP-conjugated goat anti-mouse antibody at a 1:5,000 dilution for 40 min at room temperature. After being washed three times in TBS-T, the membrane was incubated with SuperSignal West Pico chemiluminescent substrate (Pierce) for 5 min and exposed to X-ray film.

Computational Analysis. Chemoreceptors were identified by searching the NCBI nonredundant database (May 7, 2009) for matches to the Pfam (9) MCPsignal domain profile (accession PF00015) with HMMER2 (10). PAS domains were identified by integrating the results of HMMER2 searches with the Pfam PAS clan profiles and SMART PAS/PAC profiles (11). Additional PAS domains were detected by BLAST searches with previously recognized PAS domains against the full-length chemoreceptor sequences. Sequences of PAS domains with known cofactors were downloaded from the nonredundant protein database. Multiple sequence alignments (MSA) were constructed using Kalign (12) and MAFFT (13) and edited using the VISSA technique (14). Conserved positions in MSA were revealed using Nigel Brown's CONSENSUS script (available at http://coot.embl.de/Alignment/consensus.html). Neighbor-joining phylogenetic trees were built from the edited MSA with MEGA4 (15). Sequence logos were generated using WebLogo (16).

Statistical Analysis of Data. A two-tailed *t* test, assuming equal variances, was used to determine whether the differences between the strains' behavior were statistically significant.

1. Alexandre G, Greer SE, Zhulin IB (2000) Energy taxis is the dominant behavior in *Azospirillum brasilense*. *J Bacteriol* 182:6042–6048.
2. Figurski DH, Helinski DR (1979) Replication of an origin-containing derivative of plasmid RK2 dependent on a plasmid function provided in trans. *Proc Natl Acad Sci USA* 76:1648–1652.
3. Greer-Phillips SE, Stephens BB, Alexandre G (2004) An energy taxis transducer promotes root colonization by *Azospirillum brasilense*. *J Bacteriol* 186:6595–6604.
4. Hallez R, Letesson JJ, Vandenhaute J, De Bolle X (2007) Gateway-based destination vectors for functional analyses of bacterial ORFeomes: Application to the Min system in *Brucella abortus*. *Appl Environ Microbiol* 73:1375–1379.
5. Hauwaerts D, Alexandre G, Das SK, Vanderleyden J, Zhulin IB (2002) A major chemotaxis gene cluster in *Azospirillum brasilense* and relationships between chemotaxis operons in alpha-proteobacteria. *FEMS Microbiol Lett* 208:61–67.
6. Watts KJ, Johnson MS, Taylor BL (2006) Minimal requirements for oxygen sensing by the aerotaxis receptor Aer. *Mol Microbiol* 59:1317–1326.
7. Reeve WG, Tiwari RP, Kale NB, Dilworth MJ, Glenn AR (2002) ActP controls copper homeostasis in *Rhizobium leguminosarum* bv. *viciae* and *Sinorhizobium meliloti* preventing low pH-induced copper toxicity. *Mol Microbiol* 43:981–991.
8. Van Dommelen A, Keijers V, Somers E, Vanderleyden J (2002) Cloning and characterisation of the *Azospirillum brasilense* glnD gene and analysis of a glnD mutant. *Mol Genet Genomics* 266:813–820.

9. Finn RD, et al. (2008) The Pfam protein families database. *Nucleic Acids Res* 36 (Database issue):D281–D288.
10. Eddy SR (1998) Profile hidden Markov models. *Bioinformatics* 14:755–763.
11. Letunic I, Doerks T, Bork P (2009) SMART 6: Recent updates and new developments. *Nucleic Acids Res* 37 (Database issue):D229–D232.
12. Lassmann T, Sonnhammer EL (2005) Kalign—an accurate and fast multiple sequence alignment algorithm. *BMC Bioinformatics* 6:298.
13. Katoh K, Toh H (2008) Recent developments in the MAFFT multiple sequence alignment program. *Brief Bioinform* 9:286–298.
14. Ulrich LE, Zhulin IB (2005) Four-helix bundle: A ubiquitous sensory module in prokaryotic signal transduction. *Bioinformatics* 21 (Suppl 3):iii45–iii48.
15. Tamura K, Dudley J, Nei M, Kumar S (2007) MEGA4: Molecular Evolutionary Genetics Analysis (MEGA) software version 4.0. *Mol Biol Evol* 24:1596–1599.
16. Crooks GE, Hon G, Chandonia JM, Brenner SE (2004) WebLogo: A sequence logo generator. *Genome Res* 14:1188–1190.

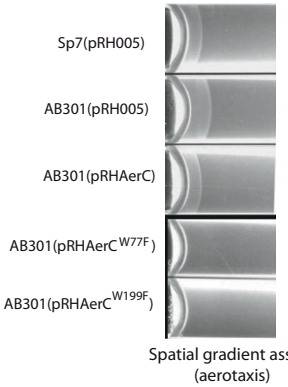

Fig. S1. An AerC–Yfp fusion expressed from the pRH005 vector complements the aerotactic defect of the AB301 strain. Mutations at conserved W77 and W199 residues in the PAS1 or PAS2 domain of AerC abolish function.

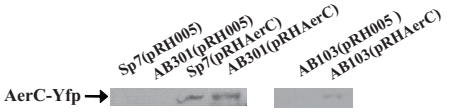

Fig. S2. Cellular levels of AerC–Yfp expressed from a low-copy vector in *A. brasilense* wild type, AB301, and AB103 mutant derivative strains. Total cellular protein extracts from *A. brasilense* wild type (Sp7), AB103, and AB301 mutant strains containing the pRH005 vectors (empty control) as well as pRHAerC expressing an AerC–Yfp fusion under the control of the native *aerC* promoter were obtained from cultures grown under conditions of nitrogen fixation. An equivalent amount of proteins (3 μg) was compared by Western blot using a rabbit monospecific polyclonal anti-GFP antibody (a gift from R. Goodchild, University of Tennessee) used at a 1:1,000 dilution.

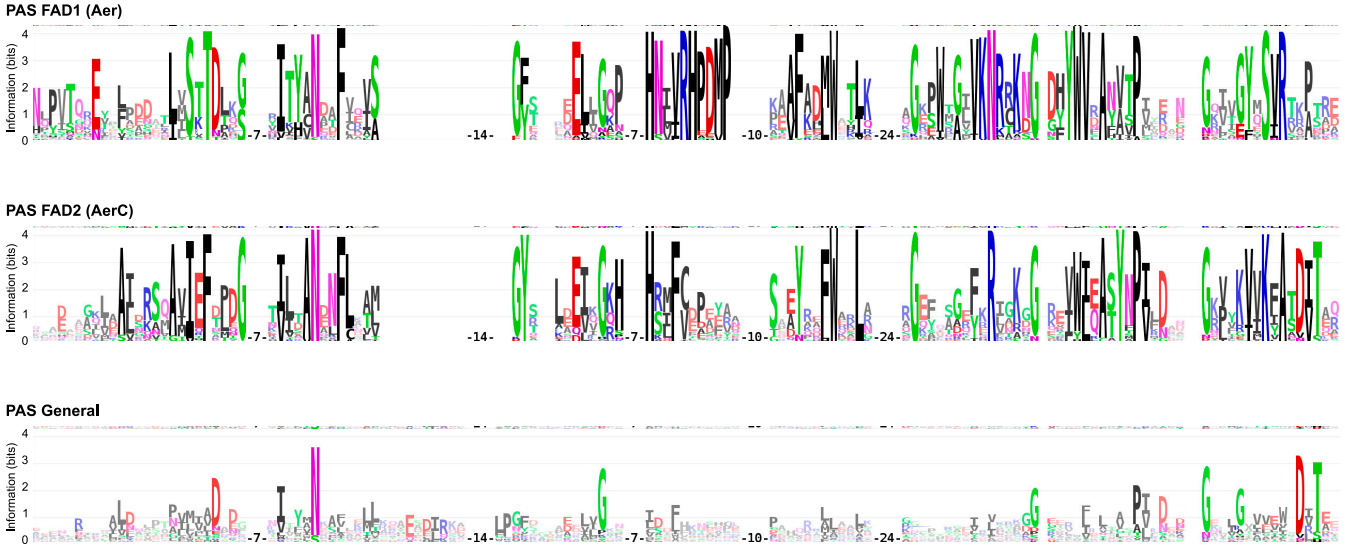

Fig. S4. Sequences logos of PAS_FAD1 and PAS_FAD2. Sequence logos of the three sequence groups revealed on the tree show strong sequence conservation between two classes and the lack of it within the general PAS group.

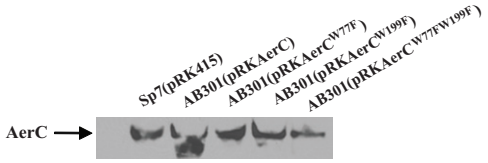

Fig. S5. Cellular levels of AerC, AerC^{W77F}, AerC^{W199F}, and AerC^{W77F199F} expressed from a low copy plasmid. Total cellular protein extracts from *A. brasilense* wild-type (Sp7) and AB301 mutant strains containing the pRK415 vectors (empty control) as well as pRKAerC, pRKAerC^{W77F}, pRKAerC^{W199F}, and pRKAerC^{W77FW199F} were obtained from cultures grown under conditions of nitrogen fixation. An equivalent amount of proteins (3 μg) was compared by Western blot using an anti-Aer$_{2-166}$ antibody from *E. coli*. The antibody was affinity purified as described in *SI Materials and Methods* and used at a 1:40 dilution. Minor degradation of AerC expressed under these conditions can be observed in the AB301 background that is not seen with AerC^{W77F}, AerC^{W199F}, or AerC^{W77F199F}.

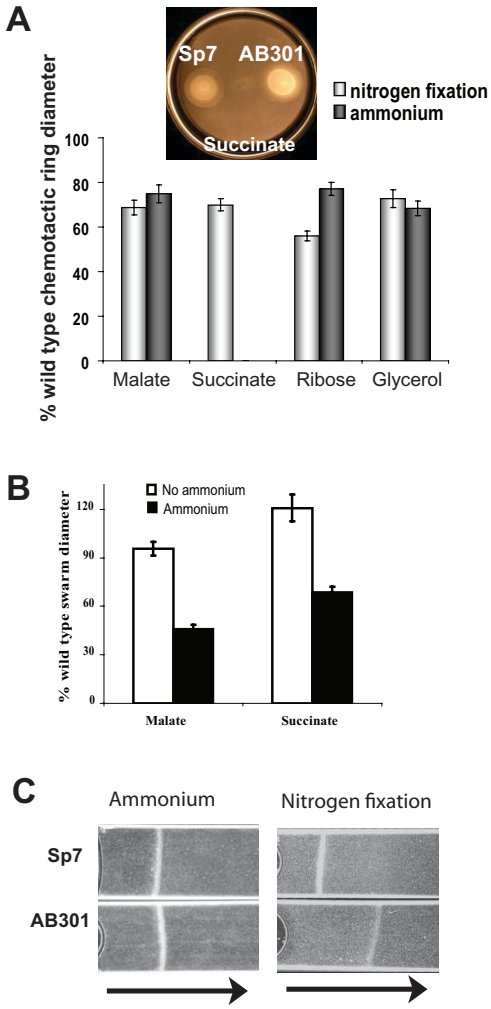

Fig. S6. Role of the AerC chemoreceptor in chemotaxis and aerotaxis. (*A*) Chemotaxis of the wild-type strain and the AB301 strain in the soft agar plate assay. The average chemotactic-ring diameters are expressed in percent relative to that the of wild-type strain (defined as 100%). Error bars represent standard deviations from the means, calculated from at least three repetitions. The chemotactic-ring diameters of AB301 were found to be significantly different from the wild-type strain with all chemoeffectors tested. The insert picture represents a soft agar plate containing succinate as the sole carbon source and ammonium. AB301 grows but does not form a chemotactic ring under these conditions. (*B*) Chemotaxis of the wild-type strain and the AB301 strain in the soft agar plate assay was tested under anaerobic conditions in minimal medium with malate or succinate (10 mM final concentration) as electron acceptors, in presence or absence of ammonium chloride and with sodium nitrate (5 mM final concentration) as the terminal electron acceptor. The average chemotactic-ring diameters are expressed in percent relative to that of the wild-type strain (defined as 100%). Error bars represent SDs from the means, calculated from at least three repetitions. (*C*) Aerotaxis of the wild-type *A. brasilense* and the AB301 strain in the capillary assay. The arrow indicates the direction of the air gradient from the air–liquid interface. Equivalent number of cells was used in the assay. The photograph was taken after 5-min incubation at room temperature.

Table S1. Total cytosolic FAD increase in wild-type *A. brasilense* on AerC overexpression

Strains	FAD increase ± SD*
Sp7(pRHAerC)	8.6124 ± 0.00695
Sp7(pRHAerC^{W77F})	3.4294 ± 0.0087†
Sp7(pRHAerC^{W199F})	2.3083 ± 0.0151†
Sp7(pRHAerC^{W77FW199F})	1.6838 ± 0.0224†

*The values of FAD increase reported are estimated as the ratio of cytosolic FAD extracted from the sample expressing AerC or its alleles normalized to the value obtained from a negative control carrying an empty vector [Sp7 (pRH005)]. Cytosolic FAD content was determined from cells grown in MMAB under nitrogen-fixation conditions by fluorometry as described in Materials and Methods. The data represent the mean values obtained from three independent cultures.

†Indicate statistically significant differences relative to Sp7(pRHAerC) in a one-way variance analysis ($P < 0.001$).

Table S2. Strains and plasmids

Strains/plasmids	Relevant characteristics	Source/reference
E. coli		
S17-1	*thi endA recA hsdR* with RP4-2Tc::Mu-K_m::Tn*7* integrated in chromosome	(1)
Top10 EC100 *pyr*	General cloning strain; *pyr*	Invitrogen Epicentre
A. brasilense		
Sp7	Wild-type strain; ATCC 29145	(2)
AB301	Δ*aerC*:: K_m derivative of Sp7;Km^r	This work
AB103 plasmids	Δ(*cheOp1*)::Cm derivative of Sp7; Cm^r	(3)
pFAJ318	pGV910 containing an *A. brasilense* P*nifH–gusA* fusion; Spc^r	(4)
pCR2.1–TOPO	PCR cloning vector, Km^r	Invitrogen
pSUP202	Suicide vector, Ap^r Tc^r Cm^r	(5)
pFUS1	pMP220 derivative containing a promoterless *gusA,* Tc^r	(6)
pFUS*aerC*	pFUS1 containing a 651-bp 5′-upstream fragment of *aerC* cloned in frame with *gusA*, yielding P*aerC–gusA* fusion, Tc^r	This work
pKNOCKTc	broad-host-range mobilizable suicide vector	(7)
pKN*aerC*UD::Kan	pKNOCKTc containing a 713-bp fragment upstream and a 699-bp fragment downstream of *aerC* and *km*^{r} cassette	This work
pCM184	Source of *km*^{r} cassette	(8)
pUC18	Cloning vector; Ap^r	(9)
pRK2013	Helper plasmid, carries *tra* genes; Km^r	(10)
pRK415	Broad-host-range vector; Tc^r	(11)
pDONR221	Km^r, Gateway entry vector	Invitrogen
pDONR*aerC*	pDONR221 with *aerC* ORF and 482-bp upstream promoter region; Km^r	This work
pDONR*aerC*^{W77F}	AerC^{W77F} and 482-bp upstream promoter region in pDONR221; Km^r	This work
pDONR*aerC*^{W199F}	AerC^{W199F} and 482-bp upstream promoter region in pDONR221; Km^r	This work
pDONR*aerC*^{W77FW199F}	AerC^{W77FW199F} and 482-bp upstream promoter region in pDNOR221; Km^r	This work
pRH005	Gateway-based destination vectors	(12)
pRHAerC	pRH005 containing a 482-bp promoter region and *aerC* ORF; Km^r Cm^r	This work
pRHAerC^{W77F}	AerC^{W77F} in pRH005; Km^r Cm^r	This work
pRHAerC^{W199F}	AerC^{W199F} and 482-bp upstream promoter region in pRH005; Km^r Cm^r	This work
pRHAerC^{W77FW199F}	AerC^{W77FW199F} and 482-bp upstream promoter region in pRH005; Km^r Cm^r	This work
pRKAerC	pRK415 containing a 2.1-kb DNA fragment encompassing promoter and *aerC* ORF	This work
pRKAerC^{W77F}	AerC^{W77F} and 482-bp upstream promoter region in pRK415; Tc^r	This work
pRKAerC^{W199F}	AerC^{W199F} and 482-bp upstream promoter region in pRK415; Tc^r	This work
pRKAerC^{W77FW199F}	AerC^{W77FW199F} and 482-bp upstream promoter region in pRK415; Tc^r	This work

Gm^r, gentamicin resistance; Km^r, kanamycin resistance; Cm^r, chloramphenicol resistance; Tc^r, tetracycline resistance; Ap^r, ampicillin.

1. Simon LD, Randolph B, Irwin N, Binkowski G (1983a) Stabilization of proteins by a bacteriophage T4 gene cloned in *Escherichia coli*. *Proc Natl Acad Sci USA* 80:2059–2062.
2. Tarrand JJ, Krieg NR, Döbereiner J (1978) A taxonomic study of the *Spirillum lipoferum* group, with descriptions of a new genus, *Azospirillum* gen. nov. and two species, *Azospirillum lipoferum* (Beijerinck) comb. nov. and *Azospirillum brasilense* sp. nov. *Can J Microbiol* 24:967–980.
3. Bible AN, Stephens BB, Ortega DR, Xie Z, Alexandre G (2008) Function of a chemotaxis-like signal transduction pathway in modulating motility, cell clumping, and cell length in the alphaproteobacterium *Azospirillum brasilense*. *J Bacteriol* 190:6365–6375.
4. Van Dommelen A, Keijers V, Somers E, Vanderleyden J (2002) Cloning and characterisation of the *Azospirillum brasilense* glnD gene and analysis of a glnD mutant. *Mol Genet Genomics* 266:813–820.
5. Simon R, Priefer U, Puhler A (1983b) A broad host range mobilization system for in vivo genetic-engineering: Transposon mutagenesis in Gram-negative bacteria. *Bio/Technology* 1: 784–791.
6. Reeve WG, Tiwari RP, Kale NB, Dilworth MJ, Glenn AR (2002) ActP controls copper homeostasis in *Rhizobium leguminosarum* bv. *viciae* and *Sinorhizobium meliloti* preventing low pH-induced copper toxicity. *Mol Microbiol* 43:981–991.

7. Alexeyev MF (1999) The pKNOCK series of broad-host-range mobilizable suicide vectors for gene knockout and targeted DNA insertion into the chromosome of gram-negative bacteria. *Biotechniques* 26:824–826, 828.
8. Marx CJ, Lidstrom ME (2002) Broad-host-range cre-lox system for antibiotic marker recycling in gram-negative bacteria. *Biotechniques* 33:1062–1067.
9. Yanisch-Perron C, Vieira J, Messing J (1985) Improved M13 phage cloning vectors and host strains: Nucleotide sequences of the M13mp18 and pUC19 vectors. *Gene* 33:103–119.
10. Figurski DH, Helinski DR (1979) Replication of an origin-containing derivative of plasmid RK2 dependent on a plasmid function provided in trans. *Proc Natl Acad Sci USA* 76:1648–1652.
11. Keen NT, Tamaki S, Kobayashi D, Trollinger D (1988) Improved broad-host-range plasmids for DNA cloning in gram-negative bacteria. *Gene* 70:191–197.
12. Hallez R, Letesson JJ, Vandenhaute J, De Bolle X (2007) Gateway-based destination vectors for functional analyses of bacterial ORFeomes: Application to the Min system in *Brucella abortus*. *Appl Environ Microbiol* 73:1375–1379.

Table S3. Oligonucleotides primers

Primer	Sequence*
tlp3UFNcoI	AATTGCCCATGGACGGCATCTTCGTCCACCG CCTTTGA
tlp3URNotI	AAATATGCGGCCGCGATGGTGCTTC
tlp3REcoRI	GGCGAATTCCGCCGACAATATGTTGC
tlp3DFApaI	AATTGCGGGCCCCAGCAACCTGATGGAATTC
tlp3DRSacI	AAATATGAGCTCCGTGGATGATGTCGAGTTC
GWTlp3F	GGGGACAAGTTTGTACAAAAAAGCAGGCTAACGCTGCCG CCATGTTC
GWTlp3R	GGGGACCACTTTGTACAAAGCTGGGTACGGGCCAACACCTTGGCG
tlp3comF	CGCAAGCTTAACGCTGCCGCCATGTTCCT
tlp3comR	GGCTCTAGATCAACGGGCCAACACCTT

*Engineered restriction sites are underlined.

Other Supporting Information Files

Fig. S3 (PDF)

Fig. S3. Domain architecture of PAS domain-containing chemoreceptors. Each chemoreceptor is identified by a GenBank Identification (GI) number (left column). Domains are from the Pfam database (1) except for PAS_FAD1, PAS_FAD2 and PAS_Gen that were built from corresponding multiple sequence alignments using the HMMER package (2). Predicted transmembrane regions are shown in blue, signal peptides in orange, coiled coil regions in green and regions of low complexity in purple.

1. Finn RD, et al. (2008) The Pfam protein families database. *Nucleic Acids Res* 36 (Database issue):D281–288.
2. Eddy S.R (1998) Profile hidden Markov models. *Bioinformatics* 14 (9):755–763.